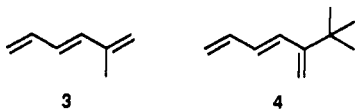


lower molar absorptivities than corresponding *s-trans* conformers. Of relevance here are *trans*-2-methyl- (3) and *trans*-2-*tert*-butyl-1,3,5-hexatriene (4), which exist predominantly in confor-



mations analogous to **1a** and **1b**, respectively.<sup>35,36</sup> Since the UV absorption spectrum of **3** has  $\epsilon = 4.3 \times 10^4 \text{ M}^{-1} \text{ cm}^{-1}$ , while the spectrum of **4** has  $\epsilon = 1.8 \times 10^4 \text{ M}^{-1} \text{ cm}^{-1}$ , both at  $\lambda_{\text{max}} = 258 \text{ nm}$ ,<sup>36</sup> it seems reasonable to expect that in the 350–380-nm region, for which  $x_2$  is nearly constant,  $1.0 \leq (\epsilon_1/\epsilon_2) \leq 3.0$ . The fluorescence quantum yield of DPH in MCH at  $T$  close to 30 °C is reported to be 0.65.<sup>27</sup> It follows that  $(\phi_1/\phi_2) \geq 0.65$ , since the fluorescence quantum yield of *s-cis*-DPH,  $\phi_2$ , cannot exceed unity. Assuming an upper limit for  $(\phi_1/\phi_2) \leq 2.0$  gives  $0.65 \leq (\epsilon_1\phi_1/\epsilon_2\phi_2) \leq 6.0$  which, on the basis of the intercept of the 355-nm plot in Figure 8, gives  $5.9 \text{ eu} \leq \Delta S_{21} \leq 10.3 \text{ eu}$  (excluding the two lowest  $T$  data points gives  $5.1 \text{ eu} \leq \Delta S_{21} \leq 9.5$ ). Since **1b** can form from **1a** in two ways, a correction of  $R \ln 2$  would have to be applied to  $\Delta S_{21}$  if the structure of *s-cis*-DPH can be assigned exclusively to **1b**.

### Conclusion

DPH fluorescence has been resolved into two components, the major of which consists of a mixture of  $2^1A_g/1^1B_u$  fluorescence spectra from the all-*s-trans* conformer **1a** and the minor of which

is a red-shifted spectrum assigned to *s-cis* conformers whose structure is most probably **1b**. Consistent with this assignment, the contribution of the red-shifted emission is enhanced by excitation at the red edge of the DPH absorption spectrum and by increasing  $T$ . Analysis of the  $T$  dependence of fractional contribution ratios of the two components in the fluorescence spectra indicates that the ground-state enthalpy difference between the conformers giving rise to these emissions is  $3.4 \pm 0.4 \text{ kcal/mol}$ , consistent with the **1a**  $\rightleftharpoons$  **1b** hypothesis.<sup>55</sup> The  $\lambda_{\text{exc}}$  dependence of the relative contribution of the two resolved spectra shows that the rotamers responsible for DPH fluorescence do not interconvert freely in the two lowest excited singlet states, thus providing strong evidence for the adherence to Havinga's NEER principle by a conjugated triene. In this regard, it would be highly surprising if selective excitation of the less favorable previtamin D<sub>3</sub> all-*s-cis* conformer shown above did not contribute, at least in part, to the pronounced  $\lambda_{\text{exc}}$  effects on photoproduct quantum yields that have been observed for previtamin D<sub>3</sub>.<sup>40,41</sup> Additional  $\lambda_{\text{exc}}$  effects due to selective formation of  $1^1B_u$  and  $2^1A_g$  states, whose different photochemical behavior competes with their equilibration, are an attractive possibility, as has been suggested.<sup>41c</sup> We have proposed a similar mechanism for the *trans*  $\rightarrow$  *cis* photoisomerization of all-*trans*-DPH,<sup>4,56</sup> and we are in the process of testing it experimentally.

**Acknowledgment.** This research was supported by NSF Grant CHE 90-14060.

**Registry No.** **1a**, 17329-15-6.

## Control of Porphyrin Orientation in Thermotropic Liquid Crystals by Molecular Design. A Time-Resolved EPR Study

Shalom Michaeli,<sup>†</sup> Muhamad Hugerat,<sup>†</sup> Haim Levanon,<sup>\*,†</sup> Mazal Bernitz,<sup>‡</sup> Aliza Natt,<sup>‡</sup> and Ronny Neumann<sup>\*,‡</sup>

*Contribution from the Department of Physical Chemistry and the Farkas Center for Light-Induced Processes and the Casali Institute of Applied Chemistry, Graduate School of Applied Science and Technology, The Hebrew University of Jerusalem, Jerusalem 91904, Israel. Received February 19, 1991. Revised Manuscript Received December 11, 1991*

**Abstract:** Molecular compatibility of a guest porphyrin in a thermotropic nematic liquid crystalline host phase was shown to control the orientation of the porphyrin chromophore. In this manner, the normal alignment of a porphyrin plane parallel to the director in a nematic phase was inverted to a perpendicular orientation by attachment of mesogenic type appendages orthogonal to a porphyrin ring on one side of the ring plane. This molecular design also leads to a head-to-tail ordering of the porphyrin even in isotropic phases. The conclusions reached are based on detection and analysis of time-resolved EPR spectra of photoexcited triplet states.

### Introduction

The study of photochemical processes in organized systems such as lyotropic and thermotropic liquid crystals are of importance owing to their relevance to such diverse fields as reaction mechanism and transport in chemical and biological systems<sup>1</sup> and the electronic and mechanical properties of synthetic liquid crystals (LC).<sup>2</sup> The former are important in the understanding of the orientation dependence of chemical reactions and of biological membrane behavior, whereas the latter are intensively being exploited for applied purposes. In recent years the chemistry of porphyrins and metalloporphyrins has attracted a great deal of attention because of the important part the porphyrin moiety plays in chemical and biological related processes, such as dioxygen and electron transfer, catalytic oxygenation,<sup>3</sup> as well as in artificial

and model photosynthesis.<sup>4</sup> Since many of these processes generally occur in organized media and not in isotropic matrices, we found it important to be able to control the orientation of a

(1) (a) Chapman, D. In *Liquid Crystals and Plastic Crystals*; Gray, G. W., Winsor, P. A., Eds.; Ellis Horwood Ltd.: Chichester, 1974. (b) Friberg, S. E. *Lyotropic Liquid Crystals Adv. Chem. Ser.* 1976, No. 152. (c) Weiss, R. G. *Tetrahedron* 1988, 44, 3413.

(2) (a) Gray, G. W. *Thermotropic Liquid Crystals*; Wiley: New York, 1987. (b) Blinov, L. M. *Electro-optical and Magneto-optical Properties of Liquid Crystals*; Wiley: New York, 1983. (c) Meier, G.; Sackmann, E.; Grabmair, J. G. *Applications of Liquid Crystals*; Springer: Berlin, 1975.

(3) (a) Collman, J. P.; Halbert, T. R.; Suslick, K. S. In *Metal Ion Activation of Dioxygen*; Spiro, T. G., Ed.; Wiley: New York, 1980; p 1. (b) Papa, S.; Lorusso, M. In NATO ASI Ser. A 76, *Biomembranes*; Butron, R. M., Guerra, F. C., Eds.; Plenum: New York, 1986; p 257. (c) Ortiz de Montellano, P. *Cytochrome P-450*; Plenum: New York, 1986.

(4) (a) Willner, I.; Willner, B. In *Topics in Current Chemistry*; Mattay, J., Ed.; Springer-Verlag: Berlin, 1991; Vol. 159, p 153. (b) Gust, D.; Moore, T. A. *Ibid.*, p 103.

<sup>†</sup> Department of Physical Chemistry and the Farkas Center.

<sup>‡</sup> Casali Institute of Applied Chemistry.

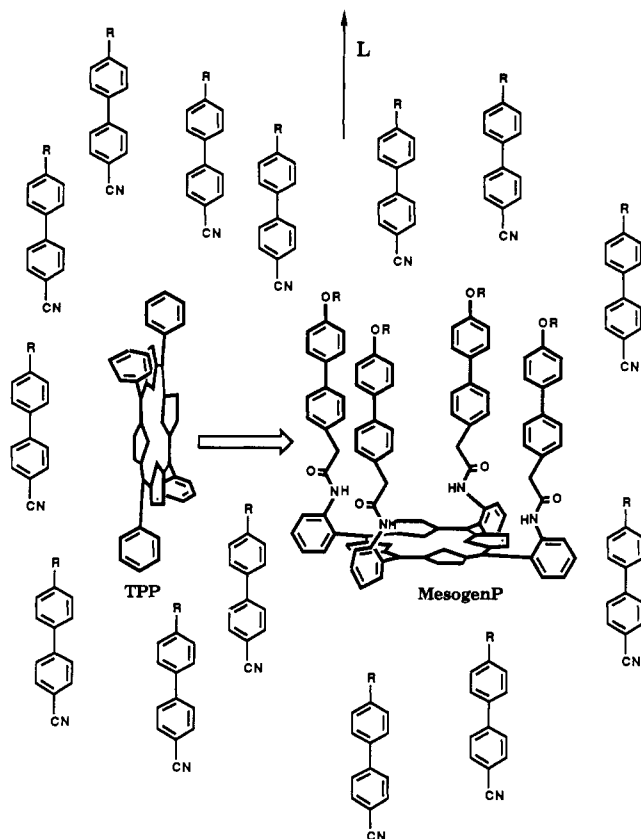


Figure 1. Orientation of TPP and MesogenP in nematic liquid crystal phase.

porphyrin within an anisotropic liquid crystalline phase, so that in the future directionality in porphyrin mediated processes may be better understood.

Therefore, the particular goal of the research described in this paper was to demonstrate such orientation control by creating a guest (porphyrin)–host (thermotropic LC) assembly<sup>5</sup> with control of the porphyrin ring orientation relative to the long axis, or director, of the LC phase. This control was attained by careful molecular design whereby mesogenic type “arms” were attached orthogonally to a porphyrin ring. Thus, 4-(4-*n*-alkoxyphenyl)phenylacetic acid was condensed with  $\alpha,\alpha,\alpha,\alpha$ -*meso*-tetrakis(*o*-aminophenyl)porphyrin, yielding as the sole product the novel porphyrins, MesogenP.<sup>6</sup> This chemical modification enables change in the orientation of the porphyrin ring from parallel (as in tetraphenylporphyrin, TPP) to perpendicular to the director, *L*, as shown in Figure 1. Furthermore, we have found that the MesogenP porphyrin is aligned in a head-to-tail fashion. The orientation of the porphyrin chromophore was studied by photoexcitation of the porphyrin in the LC assemblies. The photoexcited triplet states formed can be detected by time-resolved EPR spectroscopy and provide valuable data on molecular structure and order properties.<sup>7</sup>

## Results and Discussion

**Porphyrin Synthesis.** The porphyrins with the mesogenic “arms” or side chains were synthesized according to the reaction scheme described in Figure 2. Thus, 4-hydroxybiphenyl was etherified

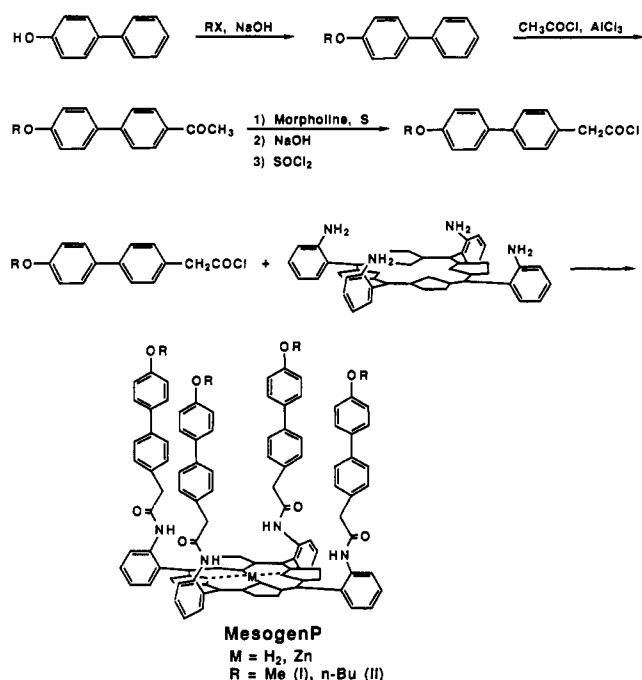


Figure 2. Reaction scheme for the preparation of MesogenP.

with dimethyl sulfate or 1-bromobutane, followed by acetylation at the 4' position, yielding the 4-acetyl-4'-*n*-alkoxybiphenyl, **1**. The latter was transformed to the required 4-(4-*n*-alkoxyphenyl)phenylacetic acid, **2**, by the Willgerodt–Kindler reaction<sup>8</sup> and condensed after preparation of the acyl chloride, **3**, derivative with the well-known  $\alpha,\alpha,\alpha,\alpha$ -*meso*-tetrakis(*o*-aminophenyl)porphyrin,<sup>9</sup> yielding the desired porphyrins with mesogenic arms, *meso*-tetra[ $\alpha,\alpha,\alpha,\alpha$ -*o*-(4-(4-*n*-alkoxyphenyl)phenylacetamido)phenyl]porphyrin, H<sub>2</sub>MesogenP-I (*R* = methyl) and H<sub>2</sub>MesogenP-II (*R* = *n*-butyl). The analogous zinc porphyrins, ZnMesogenP-I and -II, were prepared by the common metalation reaction.<sup>10</sup> The <sup>1</sup>H NMR spectra at 300 MHz (Figure 3), along with the elementary analyses (see Experimental Section), clearly identifies the compounds as the desired MesogenP porphyrins. The number of arms per porphyrin ring ratio of 4:1 is substantiated by the peak integrations, and the presence only of the  $\alpha,\alpha,\alpha,\alpha$  atropisomer is indicated by the singlet attributable to the  $\beta$ -pyrrole hydrogens. Other rotational isomers, except the very unlikely  $\alpha,\beta,\alpha,\beta$  isomer,<sup>11</sup> would show several  $\beta$ -pyrrole hydrogen peaks.

**Porphyrin Orientation in Nematic Liquid Crystal Phases.** The orientation of the porphyrin ring within the liquid crystal phase was determined by qualitative and quantitative analysis of the time-resolved EPR spectra of photoexcited triplet states. The experiments were performed by dissolving the control porphyrins (H<sub>2</sub>TPP and ZnTPP) or the MesogenP porphyrins in anisotropic nematic LC phases or in isotropic toluene solutions. Liquid crystalline solutions were heated to isotropic liquids, cooled to a nematic phase, aligned by the external magnetic field, and then frozen to 140 K, so that the liquid crystal director, *L*, can be either parallel (*L*||*B*) or perpendicular (*L*⊥*B*) to the external magnetic field, *B*.<sup>7</sup> The samples were then photoexcited by laser pulses ( $\lambda$  = 560 nm), and the resulting triplet states were detected by EPR. The resulting time-resolved triplet EPR spectra of free base porphyrins H<sub>2</sub>TPP, H<sub>2</sub>MesogenP-I, and H<sub>2</sub>MesogenP-II, and the

(5) (a) In the past, molecular compatibility with lyotropic liquid crystals has been achieved by attaching cholesteryl arms: (a) Groves, J. T.; Neumann, R. *J. Am. Chem. Soc.* **1987**, *109*, 5045. (b) Groves, J. T.; Neumann, R. *J. Am. Chem. Soc.* **1989**, *111*, 2900.

(6) Neumann, R.; Hugerat, M.; Michaeli, S.; Natt, A.; Bernitz, M.; Levanon, H. *Chem. Phys. Lett.* **1991**, *182*, 249.

(7) (a) Gonen, O.; Levanon, H. *J. Phys. Chem.* **1985**, *89*, 1637. (b) Gonen, O.; Levanon, H. *J. Chem. Phys.* **1986**, *84*, 4132. (c) Levanon, H. *Rev. Chem. Intermed.* **1987**, *8*, 287. (d) Regev, A.; Levanon, H.; Murai, T.; Sessler, J. L. *J. Chem. Phys.* **1990**, *92*, 4718. (e) Regev, A.; Galili, T.; Levanon, H. *J. Chem. Phys.*, in press.

(8) Linnell, W. H.; Smith, H. J. *J. Chem. Soc.* **1959**, 557.

(9) (a) Collman, J. P.; Gagne, R. R.; Reed, C. A.; Halbert, T. R.; Lang, G.; Robinson, W. T. *J. Am. Chem. Soc.* **1975**, *97*, 1427. (b) Lindsey, J. J. *Org. Chem.* **1980**, *45*, 5215.

(10) Fuhrop, J.-H.; Smith, K. M. *Laboratory Methods in Porphyrin and Metalloporphyrin Research*; Elsevier: New York, 1975.

(11) Since the substrate porphyrin is the  $\alpha,\alpha,\alpha,\alpha$  atropisomer and there is only one product porphyrin, the exclusive formation of the  $\alpha,\beta,\alpha,\beta$  isomer would require the extremely fortuitous rotation of two specific phenyl groups vis-à-vis the porphyrin core. Even the more likely rotation of only one random phenyl group forming the  $\alpha,\alpha,\alpha,\beta$  isomer was clearly not observed.

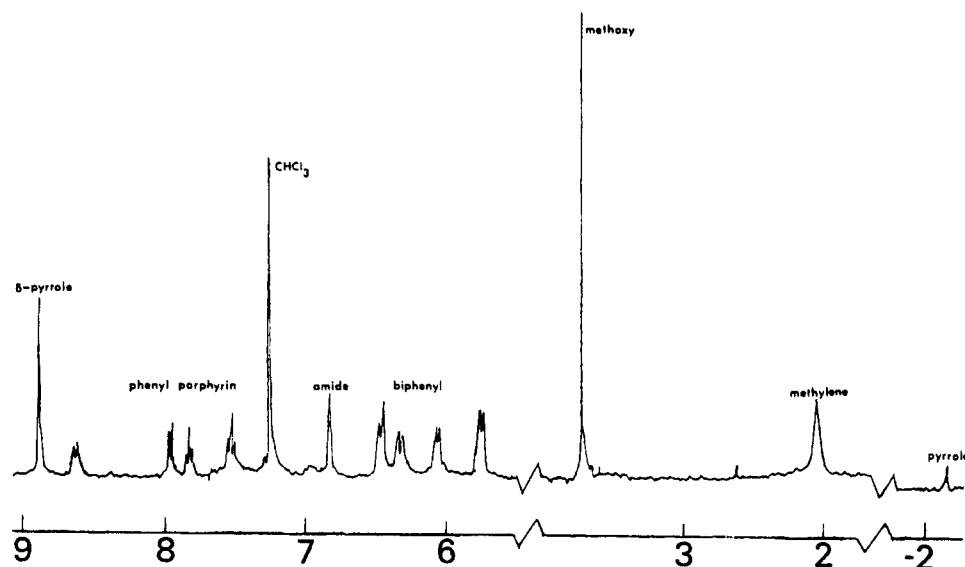


Figure 3.  $^1\text{H}$  NMR spectrum of  $\text{H}_2\text{MesogenP-I}$ .

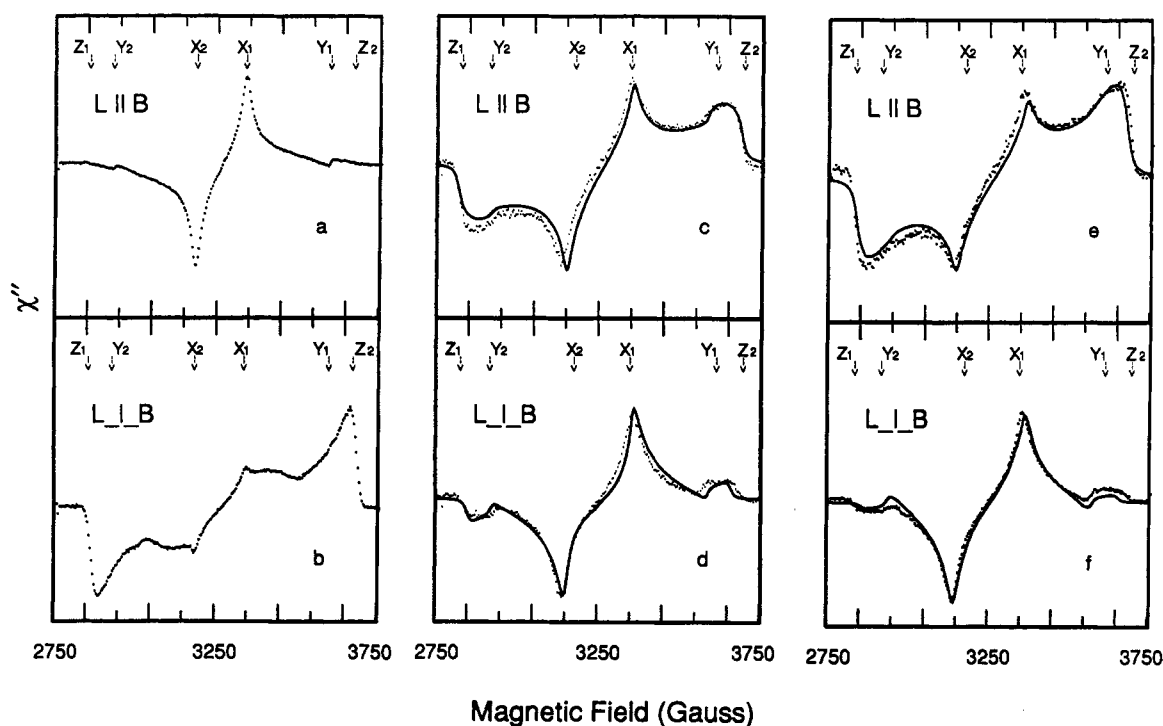


Figure 4. Direct detection, time-resolved triplet EPR spectra (parallel and perpendicular configurations) of free base porphyrins in a frozen nematic liquid crystal:  $\text{H}_2\text{TPP}$  (a, b),  $\text{H}_2\text{MesogenP-I}$  (c, d),  $\text{H}_2\text{MesogenP-II}$  (e, f). Spectra were recorded at 140 K at 10 mW microwave power, 625 ns after laser excitation pulse (25 mJ/pulse at 560 nm). The smooth curves superimposed on the experimental spectra are computer simulations (eq 5). The calculated parameters for the simulations are given in Table I and II. In the present work, no simulations were carried out for the control spectra (the parameters in Tables I and II are taken from ref 7a,b). The canonical orientations are marked by arrows.

analogous zinc porphyrins are shown in Figures 4 and 5, respectively. Qualitatively, it is clear from the experimental results (dotted lines) that the spectra of the control porphyrins in the parallel configuration ( $\text{L} \parallel \text{B}$ ) are similar to those of the MesogenP-II porphyrin in the perpendicular configuration ( $\text{L} \perp \text{B}$ ) and vice versa. On the other hand, the MesogenP-I porphyrins at each orientation show intermediate spectra, whose line shapes are spectral admixtures of the control, and the MesogenP-II porphyrins, with a closer resemblance to the MesogenP-II compounds at their respective orientations.

The interpretation of the spectra is best performed by reexamination of the triplet spectra of  $\text{H}_2\text{TPP}$  oriented in the frozen nematic phase already discussed and analyzed in the past.<sup>7b,c</sup> The spectrum in the parallel configuration (Figure 4a), characterizes an orientation where the director lies in the porphyrin ring plane, whereas the spectrum at the perpendicular configuration (Figure

4b) indicates an orientation where the director is perpendicular to the external magnetic field, and the out-of-plane, zero-field splitting (ZFS) magnetic axis,  $Z$ , is parallel to the external magnetic field. This orientation is associated with the maximum splitting of the spectrum ( $|Z_1 - Z_2| = 2D$ ). The other two principal ZFS axes,  $X$  and  $Y$ , are located on the molecular plane of the porphyrin ring, and are perpendicular to  $Z$ . These three principal axes are commonly referred to as the canonical orientations and are shown on each triplet spectrum.

Following the spectral interpretation of the known  $\text{H}_2\text{TPP}$  porphyrin, we suggest that  $\text{H}_2\text{Mesogen-I}$  and to a greater extent  $\text{H}_2\text{Mesogen-II}$  are aligned in the nematic phase (Figure 4c-f) so that the director is pointing out of the porphyrin plane, forming an angle lying between  $\pi/2$  and  $\pi/4$ . We infer this from the inversion of the spectra, keeping in mind that the basic spectroscopic properties, that is, the ground state absorption of the

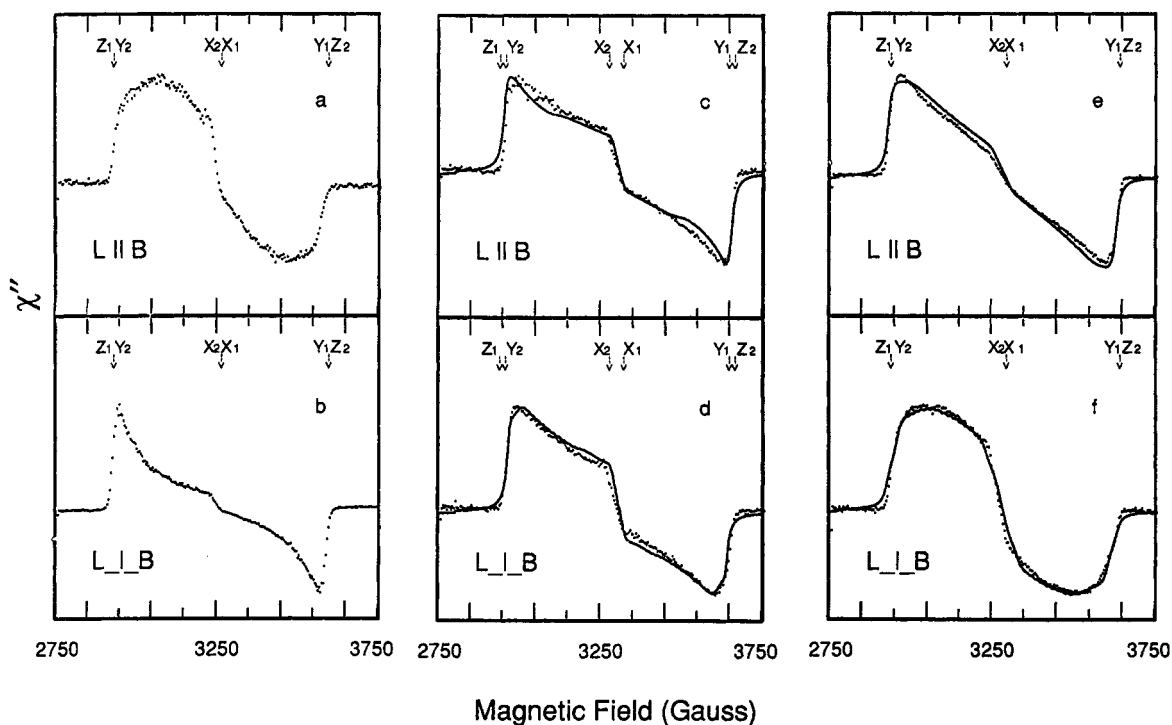


**Figure 5.** Direct detection, time-resolved triplet EPR spectra of zinc porphyrins in a frozen nematic liquid crystal: ZnTPP (a, b), ZnMesogenP-I (c, d), ZnMesogenP-II (e, f). Other conditions are as in Figure 4, except that spectra were recorded 325 ns after the laser pulse.

porphyrin ring chromophore, are identical for both systems. Thus, the possibility that the larger width of the EPR spectra of H<sub>2</sub>MesogenP in the L||B configuration, compared to the L⊥B configuration, is due to different alignment of triplet electron spins as compared to conventional porphyrins, or out-of-plane location of the optical transition moment may be ruled out in this case.<sup>12</sup> The differences in line shapes found in each case are attributed to the different angles between the director and the porphyrin plane and different fluctuations of the porphyrins around the director.<sup>7b,c</sup> The above qualitative arguments presented for the free base porphyrin may naturally be adopted for the analogous zinc porphyrins, ZnMesogenP-I and -II (Figure 5).

After the initial finding of the inversion of orientation in the frozen nematic LC state, we probed the same system in fluid nematic LC states by measuring the triplet EPR spectra of the porphyrin-LC assemblies at ambient temperatures (298 K). At this temperature the molecular ordering and fluctuations are allowed, giving a better feeling for the molecular compatibility of the porphyrin guest in the LC host. The fluidity of the system allows only the measurement of the spectrum in the parallel configuration (L||B) due to the fast motion of the director in the fluid phase within the EPR time scale, which maintains the director parallel to the external magnetic field.<sup>7d,e</sup> The spectra are shown in Figure 6, and their comparison with those of the control porphyrins in the perpendicular configuration (L⊥B) in frozen matrices (Figure 4b and 5b) again clearly shows the inversion of orientation upon addition of mesogenic arms to the porphyrin ring.

**Line-Shape Analysis.** In order to obtain a quantitative analysis of the triplet EPR spectra, a line-shape analysis of the triplet spectra was performed along the lines we have previously described.<sup>7</sup> For example, in an anisotropic environment, e.g., a LC of uniaxial symmetry, the ZFS principal axes of the guest chromophore (porphyrin ring) have different probabilities to be parallel to the external magnetic field, **B**. The experimental EPR intensity as a function of the external magnetic field is an ensemble average of the triplet signals from all the possible orientations of the

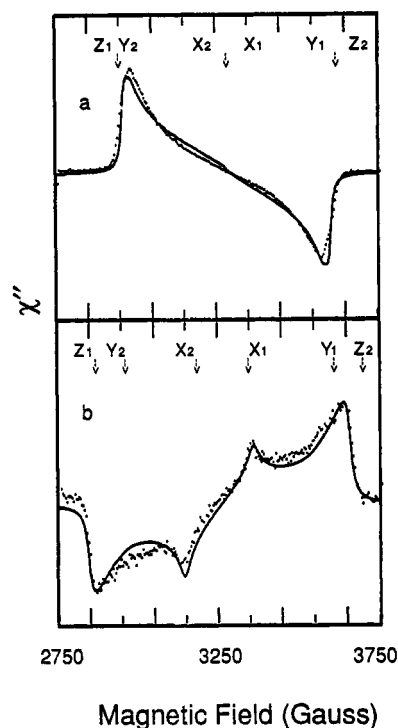


**Figure 6.** Direct detection time-resolved triplet EPR spectra (parallel configurations only) of MesogenP-II porphyrins in a fluid nematic liquid crystal: ZnMesogenP-II (a), H<sub>2</sub>MesogenP-II (b). Spectra were recorded at 298 K; other conditions as in Figures 4 and 5.

magnetic system. For the cylindrical distribution of the guest compound about the director, **L**, the EPR line shape is given by:<sup>7b</sup>

$$\chi''(\mathbf{B}, t) \propto \sum_{\substack{i=1,2 \\ j=i+1}} \int_0^{\pi/2} f(\theta') \int_{\theta_{\min}}^{\pi/2} \int_0^{\pi/2} \text{Im}[p_{ij}(\theta, \phi, t)] f(\phi) d\theta d\phi d\theta' \quad (1)$$

The functions  $f(\theta')$  and  $f(\phi)$  reflect the distributions of the guest compound about the director. The former function,

(12) For cases, where triplet spectra indicate an out-of-plane optical transition moment see, e.g.: (a) Levanon, H.; Regev, A.; Michaeli, S.; Galili, T.; Cyr, M.; Sessler, J. L. *Chem. Phys. Lett.* **1990**, *174*, 253. (b) Regev, A.; Michaeli, S.; Levanon, H.; Cyr, M.; Sessler, J. L. *J. Phys. Chem.* **1991**, *95*, 9121.

$$f(\theta') = \cos^2(\theta') \exp(-\theta'^2/\sigma_{\theta'}^2) \quad (2)$$

expresses the fluctuations of the molecular porphyrin plane about the director, and the latter function,

$$f(\phi) = \exp(-(\phi_0 - \phi)^2/\sigma_{\phi}^2) \quad (3)$$

describes the probability of the rotation of the porphyrin ring chromophore about an axis perpendicular to its molecular plane. Equation 1 is valid for any orientation of the director with respect to the external magnetic field. Here, this relative orientation is controlled by the lower integration limit,  $\theta_{\min} = \pi/2 - \chi \pm \theta'$ , where the angle  $\chi$  describes the rotation angle of **L** about **B**, and the sign of  $\theta'$  is chosen so that  $0 \leq \theta_{\min} \leq \pi/2$ . All of the experiments were carried out either at the parallel or perpendicular configuration of the director relative to the external magnetic field. Therefore, in applying eq 1, two angles of rotation are of concern, i.e.,  $\chi = 0^\circ$  (**L**||**B**) and  $\chi = 90^\circ$  (**L**⊥**B**). Likewise, the  $d\theta'$  integration is taken in the range of  $[0 - \pi/2]$  because of the cylindrical distribution of the guest compound about the director. For a further description of the triplet line-shape analysis and an explicit derivation of eq 1, the reader is referred to earlier publications.<sup>7</sup>

In principle, the line-shape analysis can provide the triplet magnetic ZFS parameters (**D** and **E**) and spin dynamics such as the relative selective intersystem crossing rates.<sup>7</sup> For the anisotropic system, one may also compute the order parameters and importantly earn a better understanding of the relationship between the magnetic and molecular frames of reference. In the present case, the MesogenP chromophores are subjected to LC forces which compete with the ordering properties of the chromophores due to the molecular structure of compound. For the hypothetical case where the mesogenic arms are infinitely long, the out-of-plane magnetic axis of the porphyrin is expected to be collinear with the director, **L**. On the other hand, for the other extreme case where the mesogenic arms are infinitely short, as in the control porphyrins, the LC's director should lie in the porphyrin plane. In both cases the chromophores are allowed to fluctuate to a certain degree. These fluctuations should depend on the particular chromophore, the length of the mesogenic arms, and temperature (see below). Therefore, we expect that MesogenP-I and -II should exhibit different triplet line shapes, and this more general case should be accounted for in the line-shape analysis.

If the guest porphyrins are ordered around some arbitrary direction **R** which forms an angle  $\theta'_0$  with the director **L** of the LC, then the Gaussian distribution function  $f(\theta')$  should be modified to the following form:<sup>13</sup>

$$f(\theta') = \cos^2(\theta'_0 - \theta') \exp[-(\theta'_0 - \theta')^2/\sigma_{\theta'}^2] \quad (4)$$

where the  $\cos^2(\theta'_0 - \theta')$  term is added to make  $f(\theta')$  vanish for the porphyrin plane (of the MesogenP) normal to **R**. In this case the cylindrical distribution will be around the direction **R**, so the integration must be performed in the range of  $[-\pi/2, \pi/2]$ . Following this modification, the angle  $\theta'_0$ , between **R** and **L**, may be derived from the simulations of the triplet EPR spectra. Similar to previous cases,  $\phi_0$  (eq 3) is the angle between the projection of **R** onto the porphyrin plane, and one of the in-plane canonical axes. The final equation, therefore, may be given by:<sup>14</sup>

$$\chi''(\mathbf{B}, t) \propto \sum_{\substack{i=1,2 \\ j=i+1}} \int_{-\pi/2}^{\pi/2} f(\theta') \int_{\theta_{\min}}^{\pi/2} \int_0^{\pi/2} \text{Im}[\rho_{ij}(\theta, \phi, t)] f(\phi) d\theta d\phi d\theta' \quad (5)$$

The parameters for the triplet state from computer simulations are summarized in Table I, and the orientation parameters are shown in Table II. The results clearly show that for the control

**Table I.** Magnetic Parameters and Relative Population Rates from Computer Simulations for the Triplet State of MesogenP and TPP, Oriented in a Nematic Liquid Crystal Phase

compound	solvent	T (K)	D <sup>a</sup>	E <sup>a</sup>	A <sub>x</sub> :A <sub>y</sub> :A <sub>z</sub>
H <sub>2</sub> MesogenP-I	toluene	140	404	70	1.00:0.60:0.35
H <sub>2</sub> MesogenP-I	LC	140	407	72	1.00:0.50:0.20
H <sub>2</sub> MesogenP-I	LC	298	393	65	1.00:0.55:0.20
ZnMesogenP-I	toluene	140	322	92	0.30:0.00:1.00
ZnMesogenP-I	LC	140	332	99	0.10:0.00:1.00
ZnMesogenP-I	LC	298	308	99	0.00:0.00:1.00
H <sub>2</sub> MesogenP-II	toluene	140	404	70	1.00:0.60:0.35
H <sub>2</sub> MesogenP-II	LC	140	392	62	1.00:0.53:0.20
H <sub>2</sub> MesogenP-II	LC	298	379	60	1.00:0.55:0.20
ZnMesogenP-II	toluene	140	322	92	0.30:0.00:1.00
ZnMesogenP-II	LC	140	332	110	0.10:0.00:1.00
ZnMesogenP-II	LC	298	300	95	0.00:0.00:1.00
ZnTPP <sup>b</sup>	LC	100	298	98	0.00:0.00:1.00
ZnTPP <sup>b</sup>	toluene	100	298	98	0.00:0.00:1.00
H <sub>2</sub> TPP <sup>b</sup>	LC	100	371	90	1.00:0.60:0.30
H <sub>2</sub> TPP <sup>b</sup>	toluene	100	383	80	1.00:0.60:0.30

<sup>a</sup> × 10<sup>4</sup> (cm<sup>-1</sup>) (in present calculations ± 5). <sup>b</sup> Taken from ref 7a,b.

**Table II.** Distributional Parameters of MesogenP and TPP Porphyrins in Nematic Liquid Crystal Phases<sup>a</sup>

compound	T (K)	θ <sub>0</sub>	σ <sub>θ</sub>	φ <sub>0</sub>	σ <sub>φ</sub>	S <sub>⊥</sub>	S <sub>  </sub>
H <sub>2</sub> MesogenP-I	140	73	30	45	45	0.71	0.43
H <sub>2</sub> MesogenP-I	298	75	20	45	45	0.84	0.43
ZnMesogenP-I	140	73	30	45	45	0.71	0.43
ZnMesogenP-I	298	75	20	45	45	0.84	0.43
H <sub>2</sub> MesogenP-II	140	80	15	45	45	0.91	0.43
H <sub>2</sub> MesogenP-II	298	86	10	45	40	0.96	0.50
ZnMesogenP-II	140	80	15	45	33	0.91	0.63
ZnMesogenP-II	298	85	10	45	45	0.96	0.43
H <sub>2</sub> TPP <sup>b</sup>	140	0	12	50	25	0.96	0.43
ZnTPP <sup>b</sup>	140	0	12	67	25	0.95	0.43

<sup>a</sup> Error in deg (± 5°). <sup>b</sup> Taken from ref 7a,b.

porphyrins<sup>7</sup> the angle  $\theta'_0$  between **L** and **R** is 0°, whereas for the porphyrin with mesogenic arms this angle increases as expected as a function of the arm length to ~73° for MesogenP-I and to ~80° for MesogenP-II at 140 K. The temperature should also affect the order properties, and, indeed, at 298 K the angle is further increased to ~75° and ~85° in the fluid nematic phase for MesogenP-I and MesogenP-II, respectively. Upon increasing the temperature, fast fluctuations of the MesogenP average out the contributions of the in-plane canonical orientations, leaving mainly the out-of-plane which is parallel to the external magnetic field, **B**. It is clear, therefore, that at a particular temperature, MesogenP-II will be better oriented than MesogenP-I as shown in Table II. The relation between **R** and **L** should also be reflected by the order parameters, in particular,  $S_{\perp}$  (order parameter for porphyrin plane relative to the director), which is most sensitive to fluctuations. Indeed, upon increasing the mesogen arms and the temperature, there is an increase in the value for  $S_{\perp}$  (Table II). The temperature dependence of the order properties, as reflected by  $\sigma_{\theta}$  and  $S_{\perp}$ , may be considered as the analogous effects of fast and slow motions (high and low temperatures) in magnetic resonance spectroscopy.<sup>15</sup>

The above results and their interpretation clearly indicate that the alignment of the MesogenP type porphyrin in a nematic liquid crystal is governed by the molecular compatibility of the mesogenic arms with the liquid crystal host phase (Figure 1). This compatibility is sufficiently energetically dominant to invert the normally observed alignment found for planar porphyrins such as H<sub>2</sub>TPP and ZnTPP.

**TPP Versus MesogenP in Isotropic Toluene Phases.** Another interesting aspect on the effect of addition of mesogenic arms to a porphyrin core concerns the question whether the MesogenP porphyrin tends to dimerize via a head-to-head orientation, or to

(13) Feller, W. *An Introduction to Probability Theory and Its Application*, 3rd ed.; Wiley: New York, 1970.

(14) Equation 5 assumes depolarization of light excitation. This is justified by the fact that magnetophotoselection experiments do not show significant line-shape dependence upon the polarization of light excitation (this is also the case for H<sub>2</sub>TPP; see ref 12b).

(15) Freed, J. H.; Nayeem, A.; Rananavare, S. B. In *The Molecular Dynamics of Liquid Crystals*; Luckhurst, G. R., Veracini, C., Eds.; Kluwer: Dordrecht, The Netherlands, in press (Chapters 1-5).

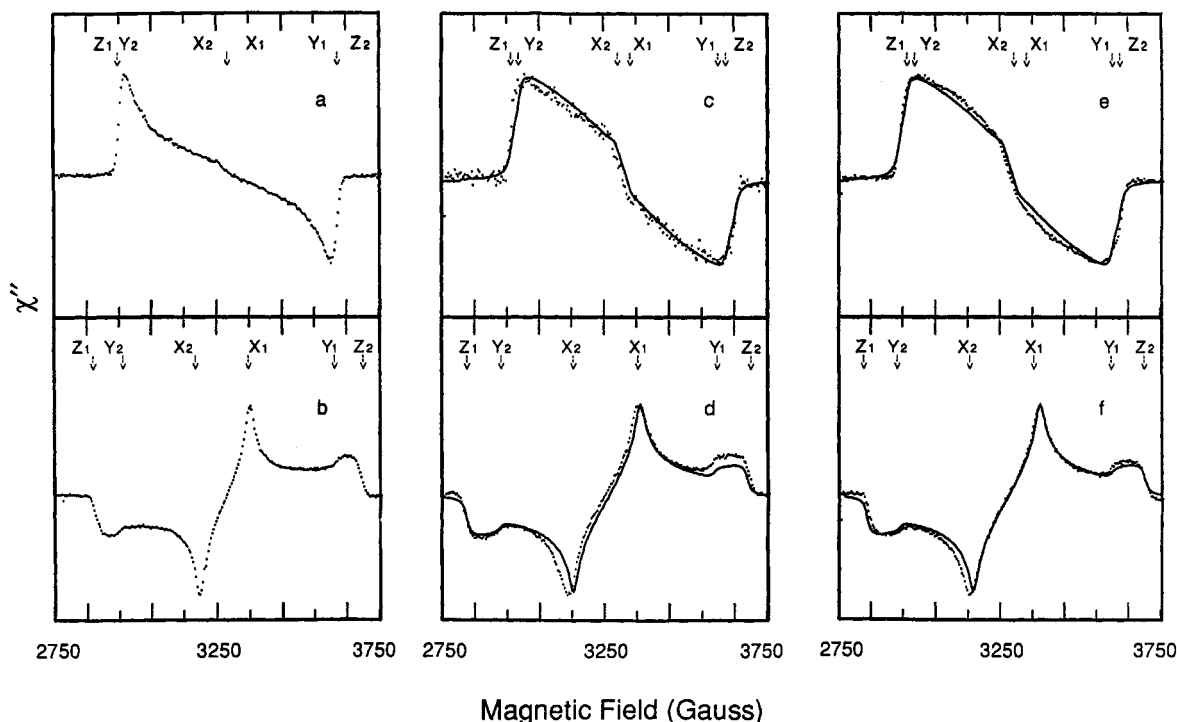


**Figure 7.** Direct detection time-resolved triplet EPR spectra of porphyrins in toluene glass: ZnTPP (a), H<sub>2</sub>TPP (b), ZnMesogenP-I (c), H<sub>2</sub>MesogenP-I (d), ZnMesogenP-II (e), H<sub>2</sub>MesogenP-II (f). Spectra were recorded at 140 K with conditions as described in Figures 4 and 5. The line-shape simulations are for randomly distributed triplets.

exist in a head-to-tail orientation. It has already been reported<sup>7b,16</sup> that ZnTPP aggregates in an isotropic matrix such as toluene to form dimers, with a face-to-face orientation, in which one monomeric constituent is rotated by  $\pi/2$  relative to its counterpart. In those previous studies,<sup>7b,16</sup> the line-shape analyses of the triplet EPR spectra were consistent with a dimeric species in which the in-plane  $X$  and  $Y$  magnetic axes of one triplet ZnTPP are exchanging energy with  $Y$  and  $X$  axes of its neighboring ZnTPP, according to the scheme:



It should be pointed out that no experimental evidence is available that H<sub>2</sub>TPP dimerizes under the same experimental conditions. To investigate the possible dimerization of the currently examined MesogenP compounds, we have recorded the spectra of the control TPP and the MesogenP compounds in an isotropic toluene glass matrix (Figure 7). It is evident that the triplet spectrum of ZnTPP is quite different from both the ZnMesogenP triplet spectra. Moreover, the triplet spectra of the two ZnMesogenP (Figure 7b,c) are identical within the experimental error. On the other hand, the triplet spectrum of H<sub>2</sub>TPP (Figure 7b) is almost identical with that of both the H<sub>2</sub>MesogenP-I and -II spectra. Recalling that H<sub>2</sub>TPP does not form triplet dimers, the latter observation in the free base compounds is easily interpreted in terms of monomeric triplet species with no indication of triplet energy transfer. However, the different triplet spectra of the zinc analogues warrants further comment. In the case of ZnTPP the intensities at the canonical orientations  $X$  and  $Y$  are appreciably reduced because of triplet exchange via the  $X$  and  $Y$  magnetic axes of the two porphyrin planes in the dimer as previously reported (Figure 7a).<sup>7b,16</sup> The triplet spectra of ZnMesogenP in toluene glass (Figure 7c,e) show all the canonical axes ( $Y$  and  $Z$  overlap, because  $D \approx 3E$ ). This indicates that energy transfer, as found for ZnTPP dimeric species, does not occur in the present case. This conclusion lends credence to a head-to-tail-type orientation, despite the fact that head-to-head orientation is still possible in a steric sense as one porphyrin face is unhindered. The solid lines superimposed on the experimental spectra are calculated

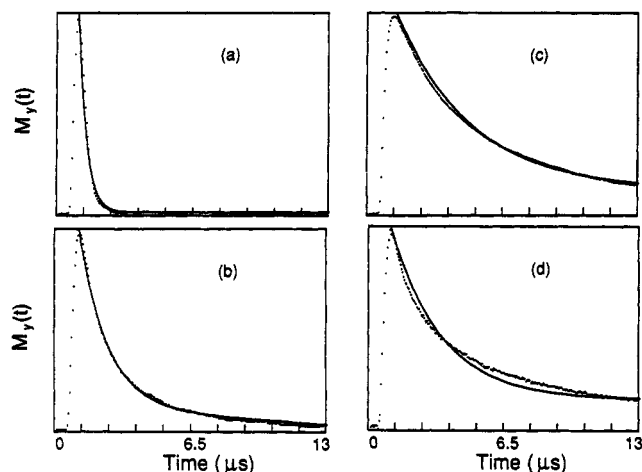


**Figure 8.** Decay rate of transverse magnetization,  $M_y(t)$ , of porphyrins in toluene glass at 140 K and 10 mW microwave power: ZnTPP (a), ZnMesogenP-II (b), H<sub>2</sub>TPP (c), H<sub>2</sub>MesogenP-II (d). The experimental curves were fitted by a single exponential decay curve.

curves using an equation for the line shape, which is similar to eq 1, but modified to an isotropic triplet distribution without energy transfer terms in it.<sup>7</sup> Supporting evidence for this monomeric species can be found by measuring the rate of decay of transverse magnetization,  $M_y(t)$ , shown in Figure 8. The decay is significantly faster for ZnTPP<sup>†</sup> ( $k = 3$  MHz) than for ZnMesogenP-II<sup>†</sup> ( $k = 0.8$  MHz), whereas the decay rate of H<sub>2</sub>TPP<sup>†</sup> ( $k = 0.35$  MHz) is comparable to that of H<sub>2</sub>MesogenP-II<sup>†</sup> ( $k = 0.45$  MHz). We conclude, therefore, that the triplets of ZnMesogenP in toluene do not interact; that is, they exist as monomers in toluene glass with a head-to-tail orientation dominating. We further surmise that this head-to-tail conformation is also present in the LC phase.

#### Experimental Section

**4-Acetyl-4'-alkoxybiphenyl (1).** 4-Methoxybiphenyl or 4-*n*-butoxybiphenyl (0.2 mol) prepared from 4-hydroxybiphenyl by the known procedure<sup>17</sup> was dissolved in 250 mL of dichloromethane. The mixture

(16) Scherz, A.; Levanon, H. *J. Phys. Chem.* **1980**, *84*, 324.

(17) Brewster, C. M.; Putman, I. V. *J. Am. Chem. Soc.* **1939**, *61*, 3082.

was cooled to 0–5 °C and 0.22 mol of  $\text{AlCl}_3$  was added, followed by dropwise addition over 0.5 h of 0.21 mol of acetyl chloride. The reaction was continued for 2 h at room temperature and treated with  $\text{HCl}$ -ice. The dichloromethane phase was dried with  $\text{Na}_2\text{SO}_4$  and the solvent evaporated. The crude product was titrated with ether and then recrystallized from ethanol yielding 24 g (53%) of **1a** ( $R = \text{Me}$ ), mp 152–3 °C (lit.<sup>18</sup> 156 °C) [Anal. Calcd for  $\text{C}_{15}\text{H}_{14}\text{O}_2$ : C, 79.62; H, 6.24; O, 14.14. Found: C, 79.8; H, 6.4], and 22 g (41%) of **1b** ( $R = n\text{-Bu}$ ), mp 136 °C.  $^1\text{H}$  NMR at 300 MHz in  $\text{CDCl}_3$ :  $\delta$  0.99 (t, 3 H), 1.47 (m, 2 H), 1.80 (m, 2 H), 2.63 (s, 3 H), 4.02 (t, 2 H), 7.01 (d, 2 H), 7.55 (d, 2 H), 7.63 (d, 2 H), 8.02 (d, 2 H). Anal. Calcd for  $\text{C}_{18}\text{H}_{20}\text{O}_2$ : C, 80.56; H, 7.51; O, 11.92. Found: C, 80.3; H, 7.42.

**4-(4-Alkoxyphenyl)phenylacetic Acid (2).** These compounds were synthesized by refluxing a mixture of 0.08 mol of **1**, 0.12 mol of sulfur, and 0.12 mol of morpholine for 14 h and then pouring this mixture into 500 mL of 15%  $\text{NaOH}$ , whereupon reflux was continued for an additional 12-h period. The solution was cooled and filtered. The solid was redissolved in boiling water and the filtrate acidified, yielding crude product **2**. The crude product was recrystallized from benzene giving a yield of 11.2 g (58%) of **2a** ( $R = \text{Me}$ ), mp 188 °C (lit.<sup>8</sup> 188 °C) [Anal. Calcd for  $\text{C}_{15}\text{H}_{14}\text{O}_3$ : C, 74.36; H, 5.82; O, 19.81. Found: C, 74.5; H, 5.7], and 6.1 g (27%) of **2b** ( $R = n\text{-Bu}$ ).  $^1\text{H}$  NMR at 300 MHz in  $\text{CDCl}_3$ :  $\delta$  0.99 (t, 3 H), 1.51 (m, 2 H), 1.79 (m, 2 H), 3.68 (s, 2 H), 4.00 (t, 2 H), 6.96 (d, 2 H), 7.33 (d, 2 H), 7.50 (2d, 4 H). Anal. Calcd for  $\text{C}_{18}\text{H}_{20}\text{O}_3$ : C, 76.03; H, 7.09; O, 16.88. Found: C, 75.9; H, 7.1.

**meso-Tetra[ $\alpha,\alpha,\alpha,\alpha$ -o-(4-(4-alkoxyphenyl)phenylacetamido)porphyrin]]porphyrin,  $\text{H}_2\text{MesogenP}$ .** Compounds **2** (10 mmol) were reacted with a 10-fold molar excess of thionyl chloride at room temperature for 12 h. The excess reagent was evaporated off and the resultant crude 4-(4-alkoxyphenyl)phenylacetyl chloride, **3**, was dissolved in dry dichloromethane (10 mL) and added to 5 mL of a solution of dichloromethane containing 0.1 mmol of  $\alpha,\alpha,\alpha,\alpha$ -meso-tetrakis(o-aminophenyl)porphyrin<sup>9</sup> and 0.5 mmol of triethylamine. The solution was kept at room temperature for 2 h, then washed with water and dried; the desired  $\text{H}_2\text{MesogenP}$  porphyrins were isolated by running a silica column with a dichloromethane:ethyl acetate 9:1 eluent ( $R_f = 0.65$ ). Yields were 120 mg for  $\text{H}_2\text{MesogenP-I}$  and 110 mg for  $\text{H}_2\text{MesogenP-II}$ .  $^1\text{H}$  NMR in  $\text{CDCl}_3$  at 300 MHz for  $\text{H}_2\text{MesogenP-I}$ :  $\beta$ -pyrrole, s,  $\delta$  8.88, 8 H; phenyl hydrogens ortho to the porphyrin ring, d,  $\delta$  8.62, 4 H; phenyl hydrogens ortho to the amide, d,  $\delta$  7.95, 4 H; the other phenyl hydrogens, t,  $\delta$  7.83, 4 H and t,  $\delta$  7.52, 4 H; amide hydrogens, s,  $\delta$  6.83, 4 H; the biphenyl hydrogens, two AB doublets,  $\delta$  6.44, 6.30, 6.05, 5.74, 32 H; the methoxy hydrogens, s,  $\delta$  3.72, 12 H; the methylene hydrogens, s,  $\delta$  2.04, 8 H; the pyrrole hydrogens, s,  $\delta$  -2.27, 2 H.  $\text{H}_2\text{MesogenP-II}$ :  $\beta$ -pyrrole, s,  $\delta$  8.92, 8 H; phenyl ortho to the porphyrin ring, d,  $\delta$  8.59, 4 H; phenyl ortho to amide, d,  $\delta$  7.98, 4 H; other phenyl, t,  $\delta$  7.87, 4 H and t,  $\delta$  7.55, 4 H; amide, s,  $\delta$  6.82, 4 H; biphenyl, two AB doublets,  $\delta$  6.50, 6.37, 6.01, 5.70, 32 H;  $\alpha$ -ether, t,  $\delta$  4.00, 8 H;  $\alpha$ -carbonyl, s,  $\delta$  2.04, 8 H;  $\beta$ -ether, m,  $\delta$  1.79, 8 H;  $\gamma$ -ether, m,  $\delta$  1.46, 8 H; methyl, t,  $\delta$  0.99, 12 H; pyrrole, s,  $\delta$  -2.30, 2 H. UV-vis of  $\text{H}_2\text{MesogenP-I}$  in toluene  $\lambda_{\text{max}}$  nm (log  $\epsilon$ ): 426 (5.34); 515 (4.11); 548 (3.50); 592 (3.78); 655 (3.28).  $\text{H}_2\text{MesogenP-II}$  in toluene,  $\lambda_{\text{max}}$  nm (log  $\epsilon$ ): 426 (5.19); 514 (4.02); 548 (3.66); 590 (3.66); 650 (3.44). Anal. ( $\text{H}_2\text{MesogenP-I}$ ) Calcd for  $\text{C}_{104}\text{H}_{82}\text{N}_8\text{O}_8$ : C, 79.49; H, 5.62; N, 7.13; O, 8.12. Found: C, 79.4; H, 5.4; N, 7.1. ( $\text{H}_2\text{MesogenP-II}$ ) Calcd for  $\text{C}_{116}\text{H}_{106}\text{N}_8\text{O}_8$ : C, 80.66; H, 6.14; N, 6.44; O, 6.76. Found: C, 80.6; H, 6.1; N, 6.2.

**meso-Tetra[ $\alpha,\alpha,\alpha,\alpha$ -o-(4-(4-alkoxyphenyl)phenylacetamidophenyl)]porphyrinzinc(II),  $\text{ZnMesogenP}$ .**  $\text{H}_2\text{MesogenP}$  (30 mg) dissolved in 3 mL of DMF, and 250 mg of zinc acetate was added. The solution was brought to reflux for 30 min, then cooled. The porphyrin was extracted into dichloromethane after addition of water; the solution was dried and the solvent evaporated, yielding 28 mg of  $\text{ZnMesogenP}$ . UV-vis of  $\text{ZnMesogenP-II}$  in toluene,  $\lambda_{\text{max}}$  (log  $\epsilon$ ): 430 (5.24); 558 (3.46). UV-vis of  $\text{ZnMesogenP-I}$ : 430 (5.30); 557 (3.61).

**EPR Experiments.** EPR samples of the various porphyrins were prepared in 4-mm o.d. Pyrex tubes by dissolving the porphyrin in toluene, evaporating the toluene from the EPR tube, and then introducing the nematic phase liquid crystal (E-7, BDH)<sup>19</sup> to concentrations of  $\sim 10^{-3}$  M followed by freeze-thaw cycles and sealing off under vacuum. Alignment at low temperature (140 K) to either the parallel or perpendicular configuration was achieved by warming the solution to an isotropic liquid at a temperature above the clearing point (338 K) and then cooling in a strong magnetic field (12 kG) into the nematic mesophase (263–338 K) at room temperature for 10 min. The sample was then quickly cooled to 140 K. Spectra taken at 298 K were prepared in a similar manner without freezing the nematic phase. The samples were excited by a dye laser (Quanta Ray PDL-1) pumped by a second harmonic of a Nd:YAG laser (Quanta Ray DCR-1A). The laser excitation pulses (10 Hz) were at the Q-band region (560 nm) for both the zinc and free-base porphyrins. Time-resolved (diode detection) CW-EPR measurements were performed using a Varian E-12 spectrometer. A more detailed description of the light excitation, signal detection, and real time data acquisition are given elsewhere.<sup>7</sup>

## Conclusion

We have synthesized a novel porphyrin with mesogenic side chains attached on one side of tetraphenylporphyrin core. By use and interpretation of photoexcited triplet EPR spectra, we have shown that the molecular compatibility of these side chains with a nematic liquid crystalline host solvent enables inversion of the orientation of the porphyrin ring in a porphyrin-thermotropic liquid crystal assembly. This inversion is reflected by change from an in-plane director alignment for TPP to a perpendicular alignment of the porphyrin ring for the MesogenP compounds. In addition, we have shown that the MesogenP porphyrin tends to align itself in a head-to-tail fashion even in isotropic liquids such as toluene. We hope that, in the future, such porphyrin-thermotropic liquid crystal assemblies will aid in monitoring orientational dependence of photochemical and other biological processes such as electron transfer reactions state in such confined assemblies.

**Acknowledgment.** This work was supported by Israel Council for Research and Development, US-Israel BSF and DFG grants. The Farkas Research Center is supported by the Bundesministerium Forschung und Technologie and the Minerva Gesellschaft für die Forschung, GmbH, FRG. We are grateful to Dr. Dan Gamliel for his valuable comments.

(19) The liquid crystal is a mixture of a R-Ph-Ph-CN where  $R = n\text{-C}_5\text{H}_{11}$  (51%),  $n\text{-C}_7\text{H}_{15}$  (25%),  $n\text{-C}_8\text{H}_{17}\text{O}$  (16%),  $n\text{-C}_7\text{H}_{15}\text{Ph}$  (8%). Transition temperatures are  $C \rightarrow N$  (263 K) and  $N \rightarrow I$  (334 K).

(18) Gray, G. W.; Hartley, J. B.; Jones, B. J. *J. Chem. Soc.* **1955**, 1412.